

Chaotic dynamics in preheating after inflation

Yoshida Jin^{1,*} and Shinji Tsujikawa^{2,†}

¹*Department of Physics, Waseda University, Okubo 3-4-1, Shinjuku, Tokyo 169-8555, Japan*

²*Department of Physics, Gunma National College of Technology, Gunma 371-8530, Japan*

(Dated: October 31, 2019)

We study chaotic dynamics in preheating after inflation in which an inflaton ϕ is coupled to another scalar field χ through an interaction $(1/2)g^2\phi^2\chi^2$. First, we estimate the amplitude of the quasi-homogeneous field χ at the end of inflation for large-field inflaton potentials $V(\phi) = V_0\phi^n$ using a Fokker-Planck approach. Unlike the case of standard linear analysis the quasi-homogeneous field χ is not strongly suppressed during inflation, which can give rise to chaos between two dynamical scalar fields. For the quartic potential ($n = 4$, $V_0 = \lambda/4$) chaos actually occurs for $g^2/\lambda \lesssim 70$ in a linear regime before which the backreaction of created particles becomes important. This analysis is supported by several different criteria for the existence of chaos. For the quadratic potential ($n = 2$) the signature of chaos is not found by the time at which the backreaction begins to work, as is similar to the case of the quartic potential with $g^2/\lambda \gg 1$.

PACS numbers: 98.80.Cq

I. INTRODUCTION

Reheating after inflation is an extremely important stage to generate elementary particles present in current universe. In the original version of the reheating scenario which is now called *old reheating*, the decay of an inflaton field is characterized by a perturbative Born process [1]. However this process is not efficient for the success of the GUT-scale baryogenesis scenario. Later it was found that the existence of a nonperturbative stage—dubbed *preheating*—can lead to an explosive particle production prior to the Born decay [2, 3, 4].

During preheating scalar particles χ coupled to the inflaton ϕ are efficiently generated by parametric resonance through an interaction $(1/2)g^2\phi^2\chi^2$. The existence of the preheating stage provides several interesting possibilities such as the GUT-scale baryogenesis [5], nonthermal phase transition [6], the enhancement of metric perturbations [7] and the formation of primordial black holes [8]. In the chaotic inflationary scenario characterized by the potential $V(\phi) = V_0\phi^n$, the field perturbations $\delta\chi$ obey the Mathieu equation (for $n = 2$) or the Lame equation (for $n = 4$), which determines the structure of resonance at the linear regime. When the backreaction of created particles begins to violate the coherent oscillation of ϕ , this tends to work to suppress exponential growth of the field fluctuations. The system enters a fully nonlinear stage after which the mode-mode coupling (rescattering) between perturbations is crucially important [9, 10].

Typically the contribution of the dynamical background field χ is neglected in standard analysis of particle creations in preheating. This may be justified in linear perturbation theory, since super-Hubble perturbations in χ are exponentially suppressed during inflation for the

coupling g required for preheating [11]. However if we account for the effect of quantum diffusion using a Fokker-Planck approach [12, 13, 14], the probability distribution of the field χ has a variance that does not exhibit an exponential suppression [15]. This implies that the quasi-homogeneous field χ can play an important role for the dynamics of preheating. In fact Podolsky and Starobinsky [15] pointed out that chaos may occur for the self-coupling potential $V(\phi) = (1/4)\lambda\phi^4$ when the coupling g^2/λ is not too much larger than of order unity. Since it is not obvious whether chaos actually occurs or not in this model only by analytic estimations, we shall perform detailed numerical investigation with/without the back-reaction effect of created particles. We will use several different methods to judge the existence of chaos—such as the Toda-Brumer test [16, 17], Lyapunov exponents [18] and a fractal map [19].

It was already found that chaos appears for hybrid-type inflation models [20, 21, 22, 23] (see also Refs. [24, 25]). Hybrid inflation is a rather special model in a sense that the symmetry breaking field automatically grows by tachyonic instability even if it is suppressed during inflation. The necessary condition for chaos is that there exist at least two dynamical fields and neither of them is too much smaller than another field. The hybrid model satisfies this condition, since two fields can have frequencies which are the same order after symmetry breaking. The presence of mixing terms between two fields leads to a new instability of perturbations in addition to tachyonic/resonance instabilities [22]. This new type of instability is clearly associated with the presence of chaos.

In this work we shall investigate the existence of chaos for large-field potentials $V(\phi) = V_0\phi^n$ with an interaction $(1/2)g^2\phi^2\chi^2$. We estimate the variance of the probability distribution of χ at the end of inflation, which is relevant to the initial condition of the quasi-homogeneous field χ for preheating. The field χ is amplified by parametric resonance, which can give rise to chaos after χ grows to satisfy the Toda-Brumer condition. We shall numeri-

*Electronic address: jin@gravity.phys.waseda.ac.jp

†Electronic address: shinji@nat.gunma-ct.ac.jp

cally solve background equations together with perturbed equations for both quartic ($n = 4$) and quadratic ($n = 2$) potentials. Our main interest is to find the signature of chaos and the parameter range of the coupling g in which chaos can be seen before the backreaction effect of created particles becomes important. Since chaos can alter the standard picture of preheating by parametric resonance, it is of interest to clarify the situation in which chaos appears.

II. THE QUASI-HOMOGENEOUS FIELD χ AT THE END OF INFLATION

In this section we shall estimate the variance of the probability distribution for the field χ coupled to the inflaton ϕ through an interaction $(1/2)g^2\phi^2\chi^2$. The effective potential in our system is

$$V(\phi, \chi) = V_0\phi^n + \frac{1}{2}g^2\phi^2\chi^2. \quad (1)$$

We are mainly interested in two inflaton potentials: (i) the quadratic one ($n = 2$) and (ii) the quartic one ($n = 4$). In this work we do not implement nonminimal couplings [26] between the field χ and the scalar curvature R .

In order to estimate the field variance of χ at the end of inflation, we use the stochastic inflation approach developed by Starobinsky [12]. The Fokker-Planck equation in a de-Sitter background is given by [12, 13, 14]:

$$\frac{\partial P(\chi, t)}{\partial t} = \frac{H^3}{8\pi^2} \frac{\partial^2}{\partial \chi^2} P(\chi, t) + \frac{1}{3H} \frac{\partial}{\partial \chi} \left[\frac{\partial V}{\partial \chi} P(\chi, t) \right], \quad (2)$$

where H is the Hubble rate and $P(\chi, t)$ is the probability of observing the field χ at cosmic time t . When the probability distribution is a Gaussian, i.e.,

$$P(\chi, t) = \frac{1}{\sqrt{2\pi}\sigma(t)} \exp \left[-\frac{\chi^2}{2\sigma^2(t)} \right], \quad (3)$$

it is easy to get the following equation of motion

$$\frac{d}{dt}\sigma^2 = \frac{H^3}{4\pi^2} - \frac{2m_\chi^2(t)}{3H}\sigma^2, \quad (4)$$

where $m_\chi^2 \equiv V_{\chi\chi}$. The variance σ characterizes a typical size of the quasi-homogeneous field χ . The first term on the r.h.s. of Eq. (4) newly appears in the context of stochastic inflation because of the effect of quantum diffusion. In the absence of this term, σ exhibits exponential suppression for $m_\chi^2 \gg H^2$.

In a flat Friedmann-Lemaitre-Robertson-Walker (FLRW) background with a scale factor a , the background equations for the system (1) are

$$\ddot{\phi} + 3H\dot{\phi} + V_\phi = 0, \quad (5)$$

$$\ddot{\chi} + 3H\dot{\chi} + V_\chi = 0, \quad (6)$$

$$H^2 = \frac{\kappa^2}{3} \left[\frac{1}{2}\dot{\phi}^2 + \frac{1}{2}\dot{\chi}^2 + V(\phi, \chi) \right], \quad (7)$$

where $V_\phi = nV_0\phi^{n-1} + g^2\chi^2\phi$, $V_\chi = g^2\phi^2\chi$ and $\kappa^2 = 8\pi/m_p^2$ with m_p being the Planck mass.

We define the number of e -folds before the end of inflation, as

$$N \equiv \ln(a_f/a(t)), \quad (8)$$

where a_f is the scale factor at the end of inflation. Employing the slow-roll approximation, $|\ddot{\phi}| \ll |3H\dot{\phi}|$ and $\dot{\phi}^2 \ll V(\phi)$, we easily find that $d\phi/dN = n/(\kappa^2\phi)$. Here we neglect the contribution coming from the χ -dependent terms. Integrating this equation, we obtain

$$\phi^2 - \phi_f^2 = \frac{2n}{\kappa^2}N. \quad (9)$$

The field value at the end of inflation (ϕ_f) is determined by setting the slow-roll parameter, $\epsilon \equiv (1/2\kappa^2)(V_\phi/V)^2$, is unity. This gives $\phi_f/m_p = n/(4\sqrt{\pi})$, thereby leading to¹

$$\phi^2 = \frac{n}{4\pi} \left(N + \frac{n}{4} \right) m_p^2. \quad (10)$$

Introducing a dimensionless quantity, $z \equiv \pi\sigma^2/m_p^2$, the Fokker-Planck equation (4) can be written in the form

$$\frac{dz}{dN} + P(N)z = Q(N), \quad (11)$$

where

$$P(N) = -\frac{g^2m_p^2}{4\pi V_0} \left[\frac{nm_p^2}{4\pi} \left(N + \frac{n}{4} \right) \right]^{(2-n)/2}, \quad (12)$$

$$Q(N) = -\frac{2V_0}{3m_p^4} \left[\frac{nm_p^2}{4\pi} \left(N + \frac{n}{4} \right) \right]^{n/2}. \quad (13)$$

The solution for Eq. (11) is expressed as

$$z = \exp \left(- \int P(N)dN \right) \times \left[C + \int dN Q(N) \exp \left(\int P(N)dN \right) \right], \quad (14)$$

where C is an integration constant.

When $n = 2$ and $V_0 = m^2/2$, we obtain the following solution

$$z = e^{\frac{g^2Nm_p^2}{2\pi m^2}} \left[C + \frac{1}{3g^2} \left(\frac{m}{m_p} \right)^4 \times \left\{ N + \frac{1}{2} + \frac{2\pi}{g^2} \left(\frac{m}{m_p} \right)^2 \right\} e^{-\frac{g^2Nm_p^2}{2\pi m^2}} \right], \quad (15)$$

¹ Note that we implement the field value ϕ_f at the end of inflation unlike in Ref. [15], since this gives a non-negligible contribution to estimate the variance of χ .

where we used the slow-roll solution (10). If one takes the initial condition: $z = 0$ at $N_i = 0$, the coefficient C is determined to be

$$C = -\frac{1}{3g^2} \left(\frac{m}{m_p} \right)^4 \left\{ N_i + \frac{1}{2} + \frac{2\pi}{g^2} \left(\frac{m}{m_p} \right)^2 \right\} e^{-\frac{g^2 N_i m_p^2}{2\pi m^2}}. \quad (16)$$

When $n = 4$ with $V_0 = \lambda/4$, we get

$$z = C(N + 1)^{g^2/\lambda} - \frac{\lambda(N + 1)^3}{6\pi^2(3 - g^2/\lambda)}, \quad (17)$$

where the coefficient C corresponding to the solution $z = 0$ at $N = N_i$ is

$$C = \frac{\lambda(N_i + 1)^{3-g^2/\lambda}}{6\pi^2(3 - g^2/\lambda)}. \quad (18)$$

By the above equations one can estimate the amplitude of z at the end of inflation ($N = 0$), as

$$z_f = \frac{1}{3g^2} \left(\frac{m}{m_p} \right)^4 \left[\frac{1}{2} + \frac{2\pi}{g^2} \left(\frac{m}{m_p} \right)^2 - \left\{ N_i + \frac{1}{2} + \frac{2\pi}{g^2} \left(\frac{m}{m_p} \right)^2 \right\} e^{-\frac{g^2 N_i m_p^2}{2\pi m^2}} \right], \quad (19)$$

for $n = 2$, and

$$z_f = \frac{\lambda}{6\pi^2(3 - g^2/\lambda)} \left[(N_i + 1)^{3-g^2/\lambda} - 1 \right], \quad (20)$$

for $n = 4$.

For the quadratic potential ($n = 2$) the inflaton mass is constrained to be $m \simeq 10^{-6}m_p$ from the COBE normalization [27]. Then z_f is the function in terms of g and N_i . In Fig. 1 we plot the variance σ_f/m_p ($= \sqrt{z_f/\pi}$) at the end of inflation as a function of g for several different values of N_i . We find that σ_f is independent of the number of e -folds for $g \gtrsim 10^{-6}$. In this region the second and third terms in the square bracket of Eq. (19) are negligible relative to the first one, which gives a simple result

$$\sigma_f \simeq \frac{1}{\sqrt{6\pi}} \frac{m^2}{gm_p}. \quad (21)$$

As is clearly seen in Fig. 1 the variance becomes smaller with the increase of g . For example we have $\sigma_f/m_p = 2.3 \times 10^{-9}$ for $g = 10^{-4}$ and $\sigma_f/m_p = 2.3 \times 10^{-13}$ for $g = 1.0$.

For the quartic potential ($n = 4$) the self-coupling λ is constrained to be $\lambda \simeq 10^{-13}$ from the COBE normalization. We are interested in the regime in which parametric resonance for the field χ occurs, i.e., $g^2/\lambda > 1$. From Fig. 2 we find some difference about the value of σ_f for the parameter range $1 < g^2/\lambda < 3$ depending on the number of e -folds, although this difference is not significant for $N_i \lesssim 100$. In this case the variance σ is not

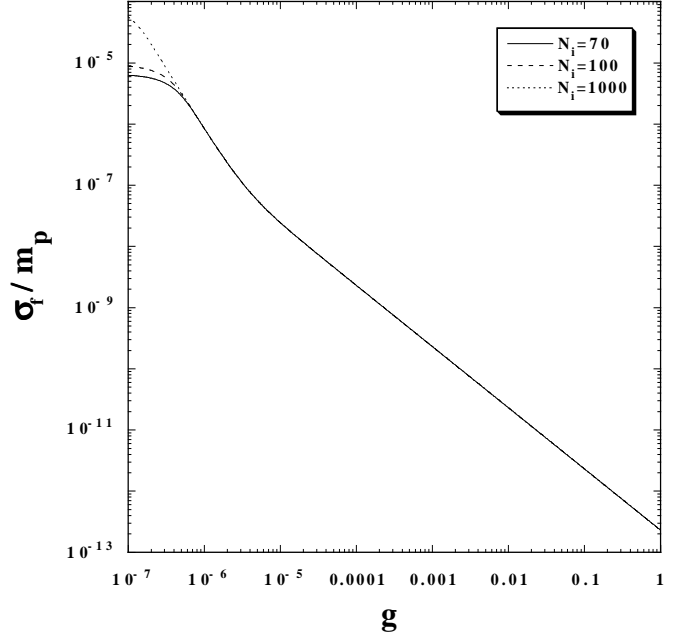


FIG. 1: The variance of the probability distribution for the field χ at the end of inflation in terms of the function of the coupling g for the quadratic potential ($n = 2$). We also show the variance for several different numbers of e -folds, i.e., $N_i = 70$, $N_i = 100$ and $N_i = 1000$. The result is not dependent on N_i for $g \gtrsim 10^{-6}$.

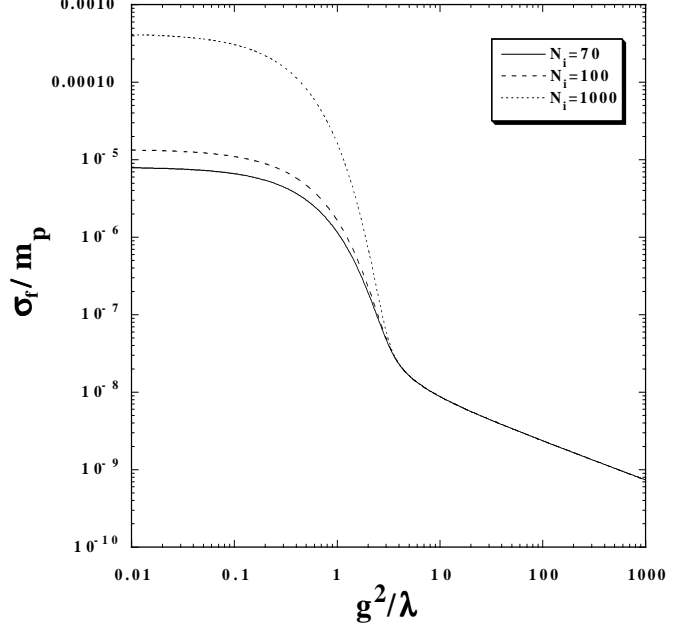


FIG. 2: The variance of the probability distribution for the field χ at the end of inflation in terms of the function of the coupling g for the quartic potential ($n = 4$). We also show the variance for several different numbers of e -folds, i.e., $N_i = 70$, $N_i = 100$ and $N_i = 1000$. The result is not dependent on N_i for $g^2/\lambda \gtrsim 3$.

strongly suppressed during inflation. Since parametric resonance occurs for $1 < g^2/\lambda < 3$, we can expect that this leads to a chaotic dynamics in terms of the two fields (ϕ and χ). In the region $g^2/\lambda \gtrsim 3$, the first term in the square bracket of Eq. (20) is negligible relative to the second term, which gives

$$\sigma_f \simeq \frac{1}{\sqrt{6\pi^3}} \frac{\lambda}{g} m_p. \quad (22)$$

This is independent of the number of e -folds, as is seen in Fig. 2. The variance σ_f decreases with the increase of g .

III. BASIC PROPERTIES OF PREHEATING AND CHAOS

A. Preheating and the role of the quasi-homogeneous field χ

In the presence of the coupling $(1/2)g^2\phi^2\chi^2$, the coherent oscillation of the inflaton leads to the excitation of the field χ during preheating through the resonance term $g^2\phi^2$ in Eq. (6). For the quadratic potential ($n = 2$) parametric resonance is efficient when the condition, $q \equiv g^2\phi^2/(4m^2) \gg 1$, is satisfied [3]. To be more precisely the field χ grows for $g \gtrsim 3.0 \times 10^{-4}$ by overcoming the friction due to cosmic expansion [10]. In this model the growth of χ ends when the system enters a narrow resonance regime ($q \lesssim 1$) or the backreaction effect of created particles breaks the coherent oscillation of the field ϕ . For the quartic potential ($n = 4$) resonance bands exist for the parameter space characterized by $n(2n-1) < g^2/\lambda < n(2n+1)$, where $n = 1, 2, 3, \dots$ [28, 29]. The center of the band, $g^2/\lambda = 2n^2$, corresponds to the largest Floquet index ($\mu_{\max} \simeq 0.28$).

If the field χ is strongly suppressed during inflation, this does not contribute to the background dynamics even if it is amplified during reheating². In standard treatment using linear perturbation theory, super-Hubble field fluctuations in χ are exponentially suppressed during inflation when the effective mass squared $m_{\text{eff}}^2 \equiv g^2\phi^2$ is much larger than H^2 [11]. In fact long wavelength modes evolve as $\delta\chi \propto a^{-3/2}$ during inflation for $g^2\phi^2 \gg H^2$, which makes the field more than 10^{-25} times smaller than its initial value when the number of e -folds is larger than $N = 60$. For the quadratic potential the condition, $g^2\phi^2 \gg H^2$, is roughly equivalent to the one under which preheating occurs, since $H \sim m$ at the end of inflation. Therefore, for the parameter range we are interested in (i.e., the field χ is amplified during preheating), χ never becomes dynamically important during preheating as long as we use standard linear analysis. Then it

is a good approximation to neglect the $g^2\chi^2\phi$ term in Eq. (5). The contribution coming from sub-Hubble fluctuations such as the $g^2\langle\delta\chi^2\rangle\phi$ term is more important, since sub-Hubble modes do not exhibit strong suppression during inflation [11].

The situation is somewhat different for the quartic potential. Parametric resonance takes place even for $g^2/\lambda = \mathcal{O}(1)$, in which case $g^2\phi^2$ is not much larger than H^2 . Therefore the field χ does not suffer from strong suppression during inflation. When $g^2/\lambda \gg \mathcal{O}(1)$ super-Hubble modes in χ are exponentially suppressed in standard linear analysis, thus dynamically unimportant during preheating.

The Fokker-Planck approach provides a good measure in estimating the amplitude of the quasi-homogeneous field χ . This gives larger values of super-Hubble modes at the end of inflation than in standard linear analysis because of the presence of diffusion terms. Then if the quasi-homogeneous field χ is amplified during preheating, this can contribute to the background dynamics significantly.

In our model the equations for field perturbations in Fourier space may be written as [15]

$$\delta\ddot{\phi}_k + 3H\delta\dot{\phi}_k + \left[\frac{k^2}{a^2} + n(n-1)V_0\phi^{n-2} + g^2\chi^2 \right] \delta\phi_k = -2g^2\phi\chi\delta\chi_k, \quad (23)$$

$$\delta\ddot{\chi}_k + 3H\delta\dot{\chi}_k + \left(\frac{k^2}{a^2} + g^2\phi^2 \right) \delta\chi_k = -2g^2\phi\chi\delta\phi_k, \quad (24)$$

where k is a comoving wavenumber. This corresponds to the equations in which the contributions from metric perturbations are dropped (see Ref. [7]). Since metric perturbations are enhanced only when field fluctuations grow sufficiently, it is a good approximation to neglect them except for a nonlinear stage of preheating.

The terms on the r.h.s. of Eqs. (23) and (24) are not usually taken into account in standard analysis of preheating [2, 3, 10], since the field χ was supposed to be dynamically unimportant. If we account for the effect of quantum diffusion, the quasi-homogeneous field χ is not exponentially suppressed during inflation, thereby giving non-negligible contributions to the r.h.s. of Eqs. (23) and (24). In fact these terms lead to a mixing between the perturbations of two fields, whose behavior is absent in standard linear analysis of preheating unless rescattering effects are taken into account at a nonlinear stage.

We start integrating background and perturbation equations from the end of inflation. The initial value of ϕ corresponds to $\phi_I/m_p = n/(4\sqrt{\pi})$, whereas we use the variance of the probability distribution of χ as the initial condition of the homogeneous field χ . We adopt the Bunch-Davies vacuum state for the initial condition of perturbations for the modes inside the Hubble radius. The total variances of the fields $\varphi = \phi, \chi$ integrated in

² The amplification of χ is limited by the backreaction effect of created particles.

terms of k are

$$\langle \delta\varphi^2 \rangle = \frac{1}{2\pi^2} \int k^2 |\delta\varphi_k|^2 dk. \quad (25)$$

We implement the variances $\langle \delta\phi^2 \rangle$ and $\langle \delta\chi^2 \rangle$ for both background and perturbation equations as a Hartree approximation [10]. We note that this is for estimating the time at which backreaction effects become important. After the system enters a fully nonlinear stage, one can not trust the analysis using the Hartree approximation. Our interest is to find a signature of chaos before the backreaction sets in.

B. The condition for chaos

In this subsection we review several conditions for the existence of chaos and apply them to our effective potential (1). Let us consider the first-order differential equations

$$\dot{x}_i = F_i(x_j), \quad (26)$$

and their linearized equations,

$$\delta\dot{x}_i = \frac{\partial F_i}{\partial x_j} \delta x_j, \quad (27)$$

where δx_i is the perturbation vector connecting two nearby trajectories and $\partial F_i/\partial x_j$ is the Jacobian matrix of $F_i(x_j)$.

The scalar-field equations (5) and (6) are expressed by the form (26) by setting $x_1 = \phi$, $x_2 = \dot{\phi}$, $x_3 = \chi$ and $x_4 = \dot{\chi}$. Then one can evaluate the Jacobian matrix $\partial F_i/\partial x_j$ and its eigenvalues μ for a general system characterized by an effective potential $V = V(\phi, \chi)$. Note that we do not account for the linearized equation for H , since metric perturbations are neglected in our analysis. The eigenvalues of the matrix $\partial F_i/\partial x_j$ are given by

$$\mu = \frac{1}{2} \left[-3H \pm \sqrt{9H^2 + 4\gamma} \right], \quad (28)$$

where

$$\begin{aligned} \gamma = & \frac{1}{2} \left[-(V_{\phi\phi} + V_{\chi\chi}) \right. \\ & \left. \pm \sqrt{(V_{\phi\phi} + V_{\chi\chi})^2 - 4(V_{\phi\phi}V_{\chi\chi} - V_{\phi\chi}^2)} \right]. \end{aligned} \quad (29)$$

The necessary condition for the existence of chaos is that one of the eigenvalues is at least positive. In an expanding background ($H > 0$) this corresponds to the condition $\gamma > 0$ from Eq. (28). Since we are now considering a situation in which both effective masses of ϕ and χ are positive ($V_{\phi\phi} > 0$, $V_{\chi\chi} > 0$), γ can take a positive value when

$$V_{\phi\phi}V_{\chi\chi} - V_{\phi\chi}^2 < 0. \quad (30)$$

This is so-called the Toda-Brumer test [16, 17] that is used to judge the existence of chaos. For our effective potential (1) this translates into the condition

$$\chi^2 > \frac{n(n-1)V_0}{3g^2} \phi^{n-2}. \quad (31)$$

When $n = 2$ and $V_0 = m^2/2$, this corresponds to

$$\chi > \frac{m}{\sqrt{3}g}, \quad (32)$$

whereas for $n = 4$ and $V_0 = \lambda/4$ we get

$$\chi > \sqrt{\frac{\lambda}{g^2}} \phi. \quad (33)$$

For the quadratic potential the initial value of χ is $m/m_p \sim 10^{-6}$ times smaller than the value which leads to chaotic instability, see Eqs. (21) and (32). Therefore the system is expected to enter a chaotic phase after the field is amplified more than 10^6 times. For the quartic potential the condition for chaos is not so severe compared to the quadratic potential, since the term on the r.h.s. of Eq. (33) decreases with time.

It is worth commenting on the difference about the instabilities of chaos and parametric resonance. Although the field χ exhibits an exponential growth by resonance, this is different from the chaotic instability in which the evolution of the system is very sensitive to slight change of initial conditions. In fact none of the eigenvalues of the Jacobi matrix is positive in the regime where the condition (31) is not satisfied. This means that chaos is absent in the region $\chi^2 < n(n-1)V_0/(3g^2)\phi^{n-2}$ even if the field shows an exponential growth by parametric resonance.

Since the Toda-Brumer test is not a sufficient condition for the existence of chaos, we shall use other criteria as well such as Lyapunov exponents [18]. The Lyapunov exponents measure the logarithm of the expansion of a small volume in a N -dimensional phase space. In this case the system possesses N Lyapunov exponents. Chaos is accompanied by an increase of the size of the N -volume at least in one direction and a maximal Lyapunov exponent h characterizes the signature of chaos. When h approaches a positive constant asymptotically, this shows the existence of chaos since the initial displacement of the N -volume grows exponentially. If h approaches to 0 asymptotically, this means the absence of chaos since the orbits are periodic or quasi-periodic. Strictly speaking Lyapunov exponents are defined in the limit $t \rightarrow \infty$. Nevertheless one can check the existence of chaos by investigating the behavior of the system for sufficiently large values of t . In fact, as we see later, the maximal Lyapunov exponent begins to grow toward a constant value when chaos appears. Although the backreaction effect of created particles can alter the background dynamics, it is possible to see the signature of chaos before the backreaction sets in.

In addition to the above two criteria, there exists another criterion for the existence of chaos— which is so

called a fractal map [19]. This strategy is useful because of gauge independence which comes from using a topological character. In the next section we shall also use this criterion to confirm the presence of chaos in addition to other methods.

IV. CHAOTIC DYNAMICS FOR THE QUARTIC POTENTIAL

For the quartic potential ($n = 4$) the system is effectively reduced to a Hamiltonian system in Minkowski spacetime by introducing conformal variables: $\tilde{\phi} \equiv a\phi$, $\tilde{\chi} \equiv a\chi$ and $\eta \equiv \int a^{-1}dt$. Using the fact that $a \propto \eta$ and $a'/a, a''/a \rightarrow 0$ during reheating in this model, the background equations (5), (6) and (7) can be written as

$$\tilde{\phi}'' + \lambda\tilde{\phi}^3 + g^2\tilde{\chi}^2\tilde{\phi} = 0, \quad (34)$$

$$\tilde{\chi}'' + g^2\tilde{\phi}^2\tilde{\chi} = 0, \quad (35)$$

$$\begin{aligned} a'^2 &= \frac{8\pi}{3m_p^2} \left(\frac{1}{2}\tilde{\phi}'^2 + \frac{1}{2}\tilde{\chi}'^2 + \frac{\lambda}{4}\tilde{\phi}^4 + \frac{g^2}{2}\tilde{\phi}^2\tilde{\chi}^2 \right) \\ &\equiv \frac{8\pi}{3m_p^2} E = \text{const}, \end{aligned} \quad (36)$$

where a prime denotes the derivative with respect to conformal time η . The trajectories of the fields are bounded by

$$\frac{\lambda}{4}\tilde{\phi}^4 + \frac{g^2}{2}\tilde{\phi}^2\tilde{\chi}^2 \leq E. \quad (37)$$

This boundary is plotted as a dotted curve in Fig. 3.

From the Toda-Brumer test (33), we can expect that chaos occurs when χ becomes comparable to ϕ for $g^2/\lambda = \mathcal{O}(1)$. When $1 < g^2/\lambda < 3$, corresponding to the first resonance band [28, 29], the variance of the field χ ranges $10^{-7} \lesssim \sigma_f/m_p \lesssim 10^{-6}$ right after the end of inflation. We require the parametric excitation of χ to give rise to chaos, since χ is much smaller than ϕ at the beginning of reheating. Therefore the coupling g needs to lie inside of the resonance band for the existence of chaos. In Fig. 3 we show an example of the background trajectory for $g^2/\lambda = 2$. We find that two fields evolve chaotically in the phase-space of the (ϕ, χ) plane by choosing several different initial conditions.

When $g^2/\lambda = 2$ the Toda-Brumer test gives the condition $\tilde{\chi}/m_p \gtrsim 0.5$ for the existence of chaos, which corresponds to the time $x \equiv \sqrt{\lambda}\phi_I\eta \gtrsim 45$ (see Fig. 4). We find that the fluctuations $\langle \delta\tilde{\chi}^2 \rangle$ and $\langle \delta\tilde{\phi}^2 \rangle$ exhibit rapid increase with a similar growth rate after the field χ satisfies the Toda-Brumer test. It is expected that this is associated with the presence of chaos rather than parametric excitation of the χ fluctuation. The quasi-homogeneous field χ is amplified by parametric resonance for $x \lesssim 45$ but stops growing after that. This comes from the fact that the resonance does not occur once the homogeneous oscillation of ϕ is broken by the growth of χ . The $g^2\phi^2$ term on the l.h.s. of Eq. (24) also becomes ineffective

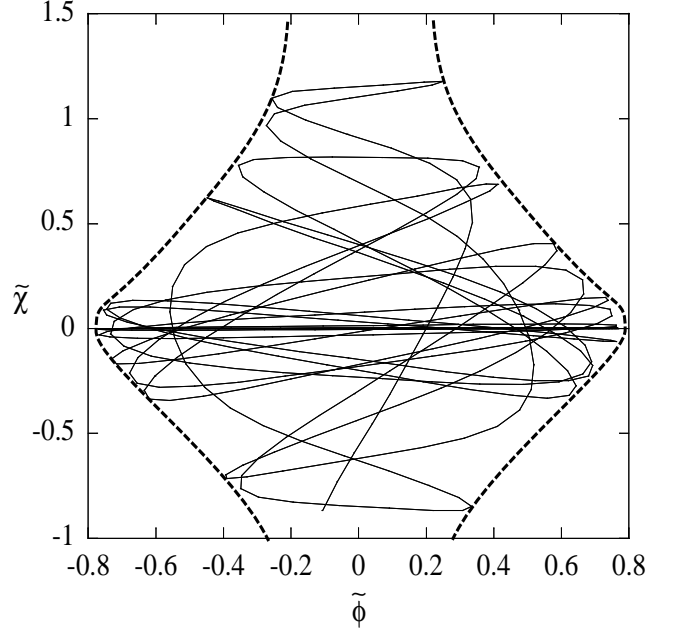


FIG. 3: A phase-space trajectory in the (ϕ, χ) plane for $g^2/\lambda = 2$. The dotted curve corresponds to the boundary given in Eq. (37).

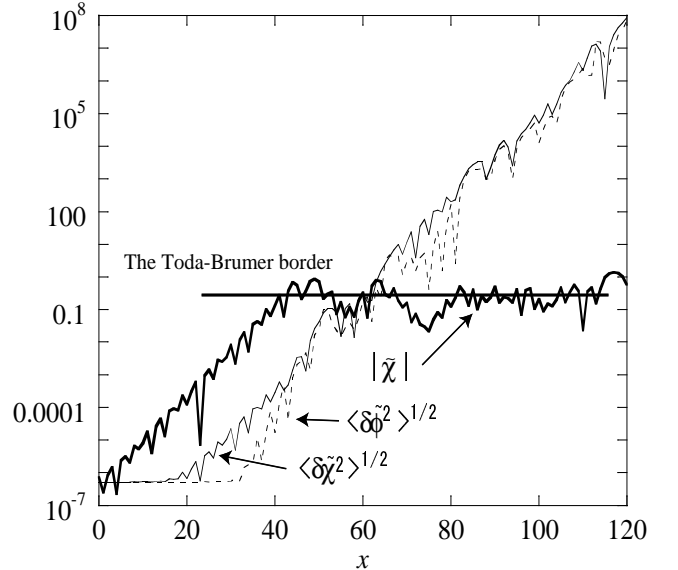


FIG. 4: Evolution of $\tilde{\chi}$, $\langle \delta\tilde{\chi}^2 \rangle^{1/2}$ and $\langle \delta\tilde{\phi}^2 \rangle^{1/2}$ (normalized by m_p) as a function of $x \equiv \sqrt{\lambda}\phi_I\eta$ for $g^2/\lambda = 2$ when the backreaction effect of created particles is neglected. The horizontal line shows the border of the Toda-Brumer test. The perturbations in ϕ and χ exhibit instabilities associated with chaos once the field χ is sufficiently amplified.

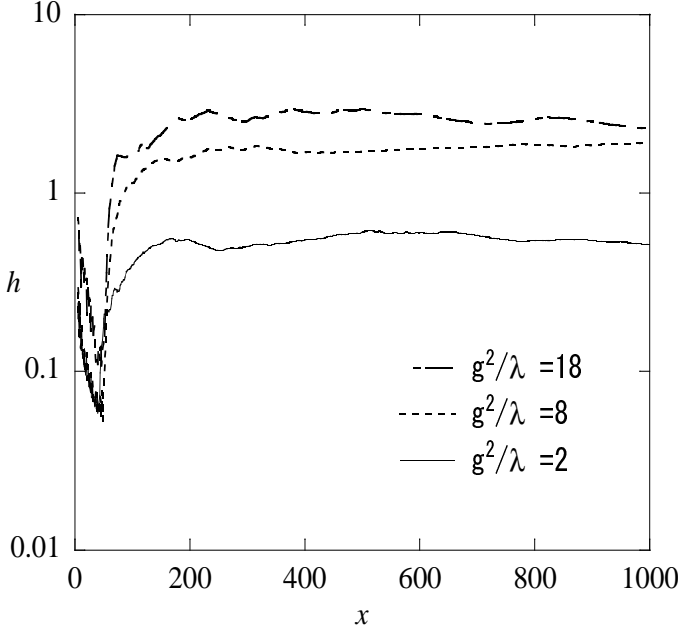


FIG. 5: Evolution of the maximal Lyapunov exponent h for $g^2/\lambda = 2, 8, 18$. We do not implement the backreaction effect of created particles. We find that the exponent h approaches a constant value in these cases.

at this stage, but the presence of the mixing term on the r.h.s. leads to a new type of instability associated with chaos. The rapid growth of $\langle \delta\tilde{\phi}^2 \rangle$ seen in Fig. 4 also comes from the mixing term on the r.h.s. of Eq. (23) rather than from the parametric excitation of the modes with $3/2 < k^2/(\lambda\phi_I^2) < \sqrt{3}$ [28, 29].

In order to check the existence of chaos, we plot the evolution of the maximal Lyapunov exponent h for several different values of g in Fig. 5. The exponent decreases at the initial stage even though χ is amplified by parametric resonance. However h begins to grow after χ satisfies the Toda-Brumer test (33). The system eventually approaches a phase with a positive constant h , which shows the existence of chaos. The growth of the maximal Lyapunov exponent is regarded as a signature of chaos, since this behavior can not be seen in the absence of chaos. We checked that h continues to decrease and converges toward 0 in power if the mixing terms do not exist on the r.h.s. of Eqs. (23) and (24).

In Fig. 6 we show a fractal map for $g^2/\lambda = 2$ with slight change of initial conditions in terms of $\tilde{\chi}_I$ and $\tilde{\chi}'_I$. We set exit pockets when the field χ becomes larger than $|\tilde{\chi}| = 1.2$. When an orbit reaches a pocket we assign colors to many initial conditions as in the following way; white if an orbit falls down to an upper pocket ($\tilde{\chi} > 1.2$), black if it falls down to a lower pocket ($\tilde{\chi} < -1.2$). Figure 6 is the result of the above manipulation, which shows that the map of initial conditions is fractal. This means that orbits are sensitive to initial data, thereby showing the existence of chaos.

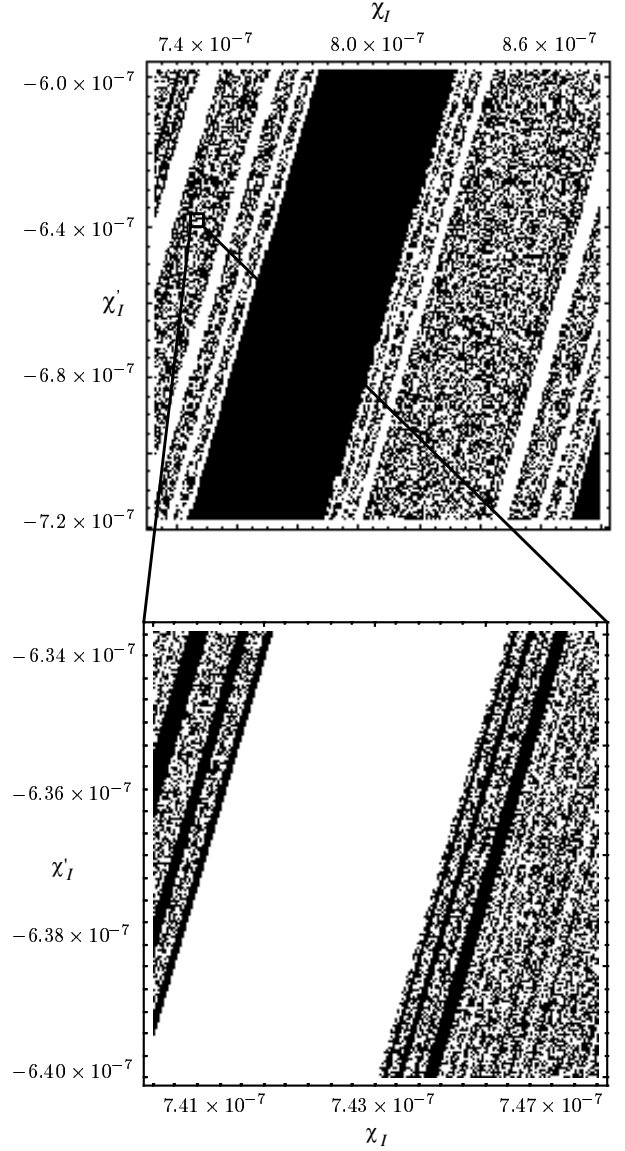


FIG. 6: A fractal map for $g^2/\lambda = 2$. We show the map of initial conditions χ_I and χ'_I with exit pockets characterized by $|\tilde{\chi}| \geq 1.2$. The white color corresponds to orbits which give $\tilde{\chi} \geq 1.2$, whereas the black one to orbits which give $\tilde{\chi} \leq -1.2$. The upper panel corresponds to the change of initial conditions by 0.1%. The lower panel is an extended figure, in which initial conditions change by 0.005%. These figures exhibit fractal structures, which result from sensitivity to initial conditions.

The above discussion neglects the backreaction effect of created particles. If we account for it as a Hartree approximation, Eqs. (5), (6), (7), (23) and (24) are modified by replacing the ϕ^2 , χ^2 and ϕ^3 terms for $\phi^2 + \langle \delta\phi^2 \rangle$, $\chi^2 + \langle \delta\chi^2 \rangle$ and $\phi^3 + 3\phi\langle \delta\phi^2 \rangle$, respectively [10]. By Eq. (23) the backreaction becomes important when

$$\sqrt{\langle \delta\tilde{\chi}^2 \rangle} \gtrsim \sqrt{\frac{3\lambda}{g^2} \tilde{\phi}}. \quad (38)$$

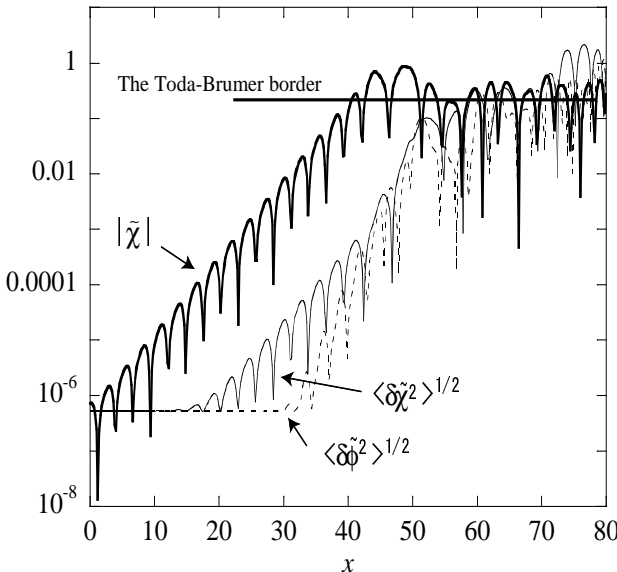


FIG. 7: Evolution of $\tilde{\chi}$, $\langle \delta\tilde{\chi}^2 \rangle^{1/2}$ and $\langle \delta\tilde{\phi}^2 \rangle^{1/2}$ (normalized by m_p) for $g^2/\lambda = 2$ when the backreaction effect is taken into account. The horizontal line corresponds to the Toda-Brumer border.

This is similar to the necessary condition for chaos for the background field χ , see Eq. (33). When $g^2/\lambda = \mathcal{O}(1)$, the Toda-Brumer test is satisfied before the condition (38) is fulfilled. This is associated with the fact that the quasi-homogeneous field χ is not strongly suppressed during inflation. As seen in Fig. 4 both $\tilde{\chi}^2$ and $\langle \delta\tilde{\chi}^2 \rangle$ have similar amplitudes initially, but the growth of sub-Hubble fluctuations occurs later than that of $\tilde{\chi}^2$. At the time when the Toda-Brumer test (33) is satisfied ($x \simeq 45$), $\langle \delta\tilde{\chi}^2 \rangle$ is much smaller than $\tilde{\chi}^2$ for $g^2/\lambda = 2$. The backreaction effect becomes important around $x = 60$ in this case.

By implementing the backreaction as a Hartree approximation, we find that this typically tends to work to suppress the growth of field fluctuations. As illustrated in Fig. 7 the fluctuations do not exhibit rapid growth after the backreaction begins to work ($x \gtrsim 60$). Nevertheless we need to caution that linear perturbation theory is no longer valid at this stage. For completeness it is required to account for the mode-mode coupling (rescattering) between the fluctuations [9]. In fact we found a numerical instability for $x \gtrsim 80$ in the simulation of Fig. 7, which signals the limitation of the Hartree approximation. It is of interest to see the effect of chaos at this fully nonlinear stage, but this is a non-trivial problem because of the complex nature of reheating. Note that the chaotic period ends at some time to complete reheating. It is difficult to judge when chaos ends in our system, since the mechanism for the decay of ϕ and χ after preheating is not completely known.

When $g^2/\lambda = \mathcal{O}(1)$ one can find out the existence of chaos during a short period before the backreaction be-

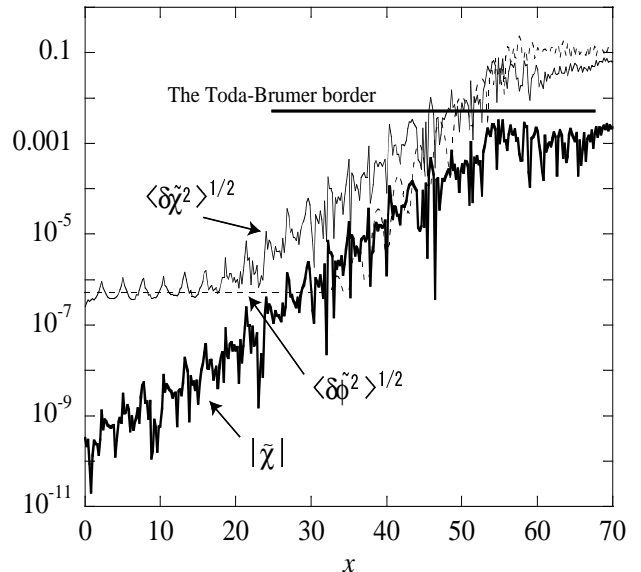


FIG. 8: As in Fig. 7 for $g^2/\lambda = 5000$.

gins to work. As we already mentioned, the criterion for chaos is given by Eq. (33), whereas the criterion for the backreaction corresponds to Eq. (38). The initial value of the quasi-homogeneous field χ gets smaller for larger g^2/λ , as illustrated in Fig. 2. This means that the condition (38) tends to be satisfied prior to the time at which the quasi-homogeneous field χ grows to satisfy the Toda-Brumer test (33). In Fig. 8 we plot the evolution of the system for $g^2/\lambda = 5000$ with the backreaction effect of created particles. In this case the backreaction becomes important around $x = 50$ before the quasi-homogeneous field χ increases sufficiently to satisfy the Toda-Brumer test. Therefore, when $g^2/\lambda \gg 1$, we do not find a signature of chaos before the perturbations reach a nonlinear regime.

We are interested in the values of g^2/λ in which chaos can be seen by the time at which the backreaction becomes important. First of all the coupling g is required to be inside of resonance bands, i.e., $n(2n-1) < g^2/\lambda < n(2n+1)$. For the coupling that belongs to these resonance bands, we find that chaos occurs for

$$g^2/\lambda \lesssim 70, \quad (39)$$

before the backreaction begins to work. When $g^2/\lambda \gtrsim 70$ the field fluctuation $\langle \delta\tilde{\chi}^2 \rangle$ satisfies the condition (38) prior to the time at which the necessary condition for chaos is fulfilled. In this case inclusion of nonlinear effects like rescattering is essentially important to understand the evolution of the two-field system and the presence of chaos. Provided that $g^2/\lambda \gg 1$, the standard Floquet theory of parametric resonance [28, 29] is valid at the linear level, since the effect of the quasi-homogeneous field χ is not important relative to its perturbations on sub-Hubble scales.

V. QUADRATIC POTENTIAL

For the quadratic potential the system can not be reduced to the analysis in Minkowski spacetime by introducing conformal quantities. Therefore the analysis in the quadratic potential is more complicated than in the case of the quartic potential in an expanding background.

We start our analysis by studying the two-field dynamics in a frictionless background. In this case the fields oscillate coherently without an adiabatic damping due to cosmic expansion. The system has the field equations corresponding to $H = 0$ in Eqs. (5) and (6) together with the constraint

$$E = \frac{1}{2}\dot{\phi}^2 + \frac{1}{2}\dot{\chi}^2 + V(\phi, \chi), \quad (40)$$

where E is conserved. Unlike the case of an expanding background, the field χ is enhanced only when the system is inside of resonance bands from the beginning of preheating. This comes from the fact that the field χ does not shift to other stability/instability bands in the absence of cosmic expansion [10]. We wish to study the existence of chaos for the coupling g that leads to parametric excitation of χ in an expanding background ($g \gtrsim 3.0 \times 10^{-4}$). First we carry out the analysis in a conserved Hamiltonian system given above and then proceed to the case in which the expansion of universe is taken into account.

We use the variance σ_f obtained in Sec. II as initial conditions of the quasi-homogeneous field χ at the beginning of preheating. As illustrated in Fig. 1 the variance is estimated to be $\sigma_f/m_p \lesssim 10^{-9}$ for the coupling $g \gtrsim 3.0 \times 10^{-4}$, which is smaller than that in the quartic potential with $g^2/\lambda = \mathcal{O}(1)$. This means that the field χ for the quadratic potential is more strongly suppressed during inflation for the values of g relevant to efficient preheating.

In Fig. 9 we plot the evolution of the background field χ together with $\sqrt{\langle \delta\chi^2 \rangle}$ and $\sqrt{\langle \delta\phi^2 \rangle}$ for the coupling $g = 3.0 \times 10^{-4}$. Note that we implement the backreaction of sub-Hubble field fluctuations as a Hartree approximation. In this case the Toda-Brumer test gives the condition $\chi/m_p > 1.9 \times 10^{-3}$ by Eq. (32). For the quadratic potential the backreaction begins to work for $\langle \delta\chi^2 \rangle \gtrsim m_p^2/g^2$, which is basically a similar condition to the Toda-Brumer test for the background field χ . As shown in Fig. 9 the quasi-homogeneous field χ does not satisfy the Toda-Brumer test, since the backreaction becomes important before χ grows sufficiently.

The variance σ_f at the end of inflation is inversely proportional to the coupling g by Eq. (21). The Toda-Brumer condition has a same property by Eq. (32). Figure 10 shows the evolution of the system for $g = 3.0 \times 10^{-3}$, in which case the quasi-homogeneous field χ is smaller relative to the case $g = 3.0 \times 10^{-4}$ by one order of magnitude. Although the condition for chaos using the Toda-Brumer test gets milder for larger g , this property is compensated by the suppression of the quasi-homogeneous field

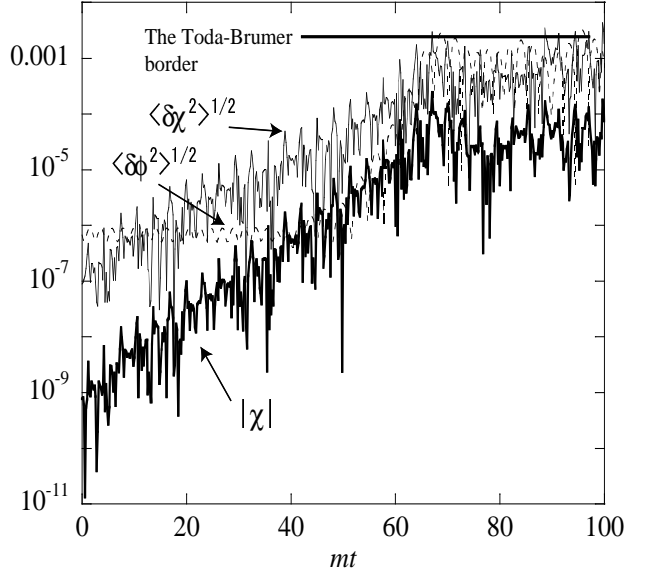


FIG. 9: Evolution of χ , $\langle \delta\chi^2 \rangle^{1/2}$ and $\langle \delta\phi^2 \rangle^{1/2}$ (normalized by m_p) for $g = 3.0 \times 10^{-4}$ without the friction due to cosmic expansion. The horizontal line represents the border of the Toda-Brumer test. We implement the backreaction effect of created particles as a Hartree approximation.

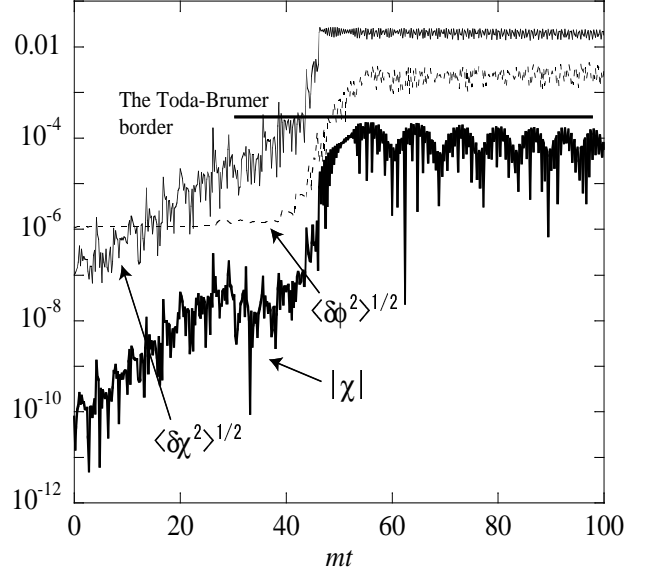


FIG. 10: As in Fig. 9 with $g = 3.0 \times 10^{-3}$.

χ at the beginning of preheating. Therefore it is difficult to satisfy the necessary condition for chaos before the backreaction begins to work. We carried out numerical simulations for other values of g and found that the signature of chaos is not seen in the frictionless system as long as the backreaction effect is taken into account.

If we implement the effect of cosmic expansion, the energy of the system given by Eq. (40) decreases. In fact

the time-derivative of E is given by

$$\frac{dE}{dt} = -3H(\dot{\phi}^2 + \dot{\chi}^2) \simeq -3HE, \quad (41)$$

where we used the approximation $E \simeq \dot{\phi}^2 + \dot{\chi}^2$. Then the energy lost during one oscillation of the inflaton ($\Delta t \simeq 1/m$) is estimated as

$$\frac{\Delta E}{E} \simeq -3 \frac{H}{m} \simeq -\sqrt{24\pi} \frac{\phi}{m_p}. \quad (42)$$

Therefore the energy loss is large at the beginning of preheating ($|\Delta E/E| \gtrsim 0.1$), but it becomes smaller and smaller with time. The analysis in the frictionless system can be used in an expanding background when the condition, $|\Delta E/E| \ll 1$, is satisfied.

In addition to the energy loss, we need to caution that the structure of resonance changes in the presence of cosmic expansion. The field χ passes many instability/stability bands, which is generally called *stochastic resonance* [10]. Parametric resonance ends when the resonance parameter, $q = g^2\phi^2/(4m^2)$, drops down to less than of order unity, whose property is different from the analysis in Minkowski spacetime.

In spite of above complexities, it is possible check whether the signature of chaos is seen or not in a linear perturbation regime. Note that the Toda-Brumer condition is valid in an expanding background. We run our numerical code including the backreaction of sub-Hubble field fluctuations for the coupling g relevant to efficient preheating ($g \gtrsim 3.0 \times 10^{-4}$) and find that the background χ stops growing by the backreaction effect before the Toda-Brumer condition is satisfied. This property is similar to the case discussed in the frictionless background. Therefore chaos does not appear for the quadratic potential at least in a regime before the backreaction sets in.

VI. CONCLUSIONS

In this paper we discussed chaotic dynamics in two-field preheating with monomial inflaton potentials $V(\phi) = V_0\phi^n$. A scalar field χ coupled to inflaton with an interaction $(1/2)g^2\phi^2\chi^2$ is amplified by parametric resonance when the inflaton oscillates coherently. As long as the background field χ is not strongly damped in an inflationary epoch, χ can grow to the same order as ϕ , thereby giving rise to a possibility of chaos during preheating.

In order to estimate the size of the quasi-homogeneous field χ at the beginning of preheating, we made use of the Fokker-Planck approach developed by Starobinsky. The variance of the probability distribution of χ grows during inflation because of the presence of the first term on the r.h.s. of Eq. (4). We derived analytic forms of the variance σ_f at the end of inflation for the effective potential $V(\phi, \chi) = V_0\phi^n + (1/2)g^2\phi^2\chi^2$. The variance

σ_f tends to be smaller with the increase of g , as shown in Figs. 1 and 2.

Since the quasi-homogeneous field χ is estimated to have an amplitude of order σ_f , we used σ_f as an initial condition of the background field χ at the beginning of preheating. Typically the homogeneous field χ is assumed to be negligible in standard analysis of particle creations in preheating, but its presence leads to a mixing between two fields. This gives rise to a chaotic instability in addition to the enhancement of perturbations by parametric resonance. The standard Floquet theory using Mathieu or Lame equation ceases to be valid when the chaos is present.

In order to study whether chaos really appears or not, we solved the background equations (5), (6) and (7) together with perturbed equations (23) and (24). For a quartic potential ($n = 4$ and $V_0 = \lambda/4$) parametric resonance can occur for the coupling g^2/λ of order unity. In this case the quasi-homogeneous field χ satisfies the Toda-Brumer test (33) before the backreaction effect of created particles becomes important. Since this is only the necessary condition for chaos, we also evaluated Lyapunov exponents for $g^2/\lambda = \mathcal{O}(1)$ in order to confirm the presence of chaos. We find that the maximal Lyapunov exponent begins to increase toward a positive constant value after the Toda-Brumer condition is satisfied, which shows the existence of chaos. Our analysis using a Fractal map also implies that the system exhibits chaotic behavior when g^2/λ is not too much larger than unity. For larger g^2/λ , the backreaction of field fluctuations on sub-Hubble scales works earlier than the time at which the Toda-Brumer test is satisfied for the background field χ . We find signatures of chaos for $g^2/\lambda \lesssim 70$ at the linear regime before the backreaction begins to work. For $g^2/\lambda \gg 1$ the quasi-homogeneous field χ gets smaller at the beginning of preheating, in which case perturbations enter a nonlinear region before chaos can be seen.

The system with a quadratic ($n = 2$) potential can not be effectively reduced to the analysis in Minkowski spacetime unlike the quartic potential. We first analyze the preheating dynamics in a frictionless background and then proceed to the case in which the expansion of universe is taken into account. In this model the background field χ does not grow sufficiently to satisfy the Toda-Brumer test in the presence of the backreaction effect of created particles. We find that this result holds both in Minkowski and expanding backgrounds. Therefore chaos can not be observed at least at the linear stage of preheating before the backreaction sets in.

In this work we did not study a nonlinear dynamics of the system during which the mode-mode coupling between perturbations plays an important role. It is of interest to investigate whether the chaotic behavior we found persists in the nonlinear regime. This can give rise to an additional instability of perturbations whose behavior is important toward complete understanding of reheating. We also note that the quartic potential is under a strong observational pressure from the require-

ment of the spectra of density perturbations even in the single-field case [30]. It will be of interest to study a non-Gaussian signature on CMB that may result from the presence of chaos in order to have a possibility to rule out this model from observations.

ACKNOWLEDGMENTS

It is a pleasure to thank Kei-ichi Maeda and Alexei Starobinsky for useful discussions. This work was par-

tially supported by a Grant for The 21st Century COE Program (Holistic Research and Education Center for Physics Self-organization Systems) at Waseda University.

[1] A. Dolgov and A. Linde, Phys. Lett. **116B**, 329 (1982); L. Abbott, E. Farhi and M. Wise, Phys. Lett. **117B**, 29 (1982).

[2] J. H. Traschen and R. H. Brandenberger, Phys. Rev. D **42**, 2491 (1990); Y. Shtanov, J. H. Traschen and R. H. Brandenberger, Phys. Rev. D **51**, 5438 (1995).

[3] L. Kofman, A. D. Linde and A. A. Starobinsky, Phys. Rev. Lett. **73**, 3195 (1994) [arXiv:hep-th/9405187].

[4] D. Boyanovsky, H. J. de Vega, R. Holman, D. S. Lee and A. Singh, Phys. Rev. D **51**, 4419 (1995) [arXiv:hep-ph/9408214].

[5] E. W. Kolb, A. D. Linde and A. Riotto, Phys. Rev. Lett. **77**, 4290 (1996) [arXiv:hep-ph/9606260]; E. W. Kolb, A. Riotto and I. I. Tkachev, Phys. Lett. B **423**, 348 (1998) [arXiv:hep-ph/9801306].

[6] L. Kofman, A. D. Linde and A. A. Starobinsky, Phys. Rev. Lett. **76**, 1011 (1996) [arXiv:hep-th/9510119]; I. I. Tkachev, Phys. Lett. B **376**, 35 (1996) [arXiv:hep-th/9510146]; S. Khlebnikov, L. Kofman, A. D. Linde and I. Tkachev, Phys. Rev. Lett. **81**, 2012 (1998) [arXiv:hep-ph/9804425].

[7] H. Kodama and T. Hamazaki, Prog. Theor. Phys. **96**, 949 (1996) [arXiv:gr-qc/9608022]; A. Taruya and Y. Nambu, Phys. Lett. B **428**, 37 (1998) [arXiv:gr-qc/9709035]; B. A. Bassett, D. I. Kaiser and R. Maartens, Phys. Lett. B **455**, 84 (1999) [arXiv:hep-ph/9808404]; M. Parry and R. Easther, Phys. Rev. D **59**, 061301 (1999) [arXiv:hep-ph/9809574]; F. Finelli and R. H. Brandenberger, Phys. Rev. Lett. **82**, 1362 (1999) [arXiv:hep-ph/9809490]; B. A. Bassett, F. Tamburini, D. I. Kaiser and R. Maartens, Nucl. Phys. B **561**, 188 (1999) [arXiv:hep-ph/9901319]; B. A. Bassett and F. Viniegra, Phys. Rev. D **62**, 043507 (2000) [arXiv:hep-ph/9909353]; F. Finelli and R. H. Brandenberger, Phys. Rev. D **62**, 083502 (2000); S. Tsujikawa and B. A. Bassett, Phys. Lett. B **536**, 9 (2002) [arXiv:astro-ph/0204031].

[8] A. M. Green and K. A. Malik, Phys. Rev. D **64**, 021301 (2001) [arXiv:hep-ph/0008113]; B. A. Bassett and S. Tsujikawa, Phys. Rev. D **63**, 123503 (2001) [arXiv:hep-ph/0008328]; F. Finelli and S. Khlebnikov, Phys. Lett. B **504**, 309 (2001) [arXiv:hep-ph/0009093]; T. Suyama, T. Tanaka, B. Bassett and H. Kudoh, arXiv:hep-ph/0410247.

[9] S. Y. Khlebnikov and I. I. Tkachev, Phys. Rev. Lett. **77**, 219 (1996) [arXiv:hep-ph/9603378]; S. Y. Khlebnikov and I. I. Tkachev, Phys. Rev. Lett. **79**, 1607 (1997) [arXiv:hep-ph/9610477].

[10] L. Kofman, A. D. Linde and A. A. Starobinsky, Phys. Rev. D **56**, 3258 (1997) [arXiv:hep-ph/9704452].

[11] P. Ivanov, Phys. Rev. D **61**, 023505 (2000) [arXiv:astro-ph/9906415]; K. Jedamzik and G. Sigl, Phys. Rev. D **61**, 023519 (2000) [arXiv:hep-ph/9906287]; S. Tsujikawa, JHEP **0007**, 024 (2000) [arXiv:hep-ph/0005105]; B. A. Bassett, M. Peloso, L. Sorbo and S. Tsujikawa, Nucl. Phys. B **622**, 393 (2002) [arXiv:hep-ph/0109176].

[12] A. A. Starobinsky, in Field Theory, Quantum Gravity, and Strings, proceedings of the Seminar, Meudon and Paris, France, 1984-1985, edited by H. T. de Vega and N. Sanchez, Lecture Notes in Physics, Vol. 246 (Springer-Verlag, New York, 1986), p 107.

[13] K. i. Nakao, Y. Nambu and M. Sasaki, Prog. Theor. Phys. **80**, 1041 (1988).

[14] D. S. Salopek and J. R. Bond, Phys. Rev. D **43**, 1005 (1991).

[15] D. I. Podolsky and A. A. Starobinsky, Grav. Cosmol. Suppl. **8N1**, 13 (2002) [arXiv:astro-ph/0204327].

[16] M. Toda, Phys. Lett. A **48** (1974) 335.

[17] P. Brumer, J. Comp. Phys. **14** (1974) 391.

[18] G. L. Baker and J. P. Gollub, *chaotic dynamics*: an introduction (Cambridge University Press, Cambridge, UK, 1996).

[19] J. D. Barrow and J. Levin, Phys. Rev. Lett. **80**, 656 (1998) [arXiv:gr-qc/9706065]; J. D. Barrow, Phys. Rept. **85** (1982) 1.

[20] R. Easther and K. i. Maeda, Class. Quant. Grav. **16**, 1637 (1999) [arXiv:gr-qc/9711035].

[21] J. Garcia-Bellido and A. D. Linde, Phys. Rev. D **57**, 6075 (1998) [arXiv:hep-ph/9711360].

[22] M. Bastero-Gil, S. F. King and J. Sanderson, Phys. Rev. D **60**, 103517 (1999) [arXiv:hep-ph/9904315].

[23] J. P. Zibin, arXiv:hep-ph/0108008.

[24] N. J. Cornish and J. J. Levin, Phys. Rev. D **53**, 3022 (1996).

[25] S. E. Joras and V. H. Cardenas, Phys. Rev. D **67**, 043501 (2003) [arXiv:gr-qc/0108088].

[26] B. A. Bassett and S. Liberati, Phys. Rev. D **58**, 021302 (1998) [Erratum-ibid. D **60**, 049902 (1999)] [arXiv:hep-ph/9709417]; S. Tsujikawa, K. i. Maeda and T. Torii, Phys. Rev. D **60**, 063515 (1999) [arXiv:hep-ph/9901306]; *ibid*, Phys. Rev. D **60**, 123505 (1999) [arXiv:hep-ph/9906501]; *ibid*, Phys. Rev. D **61**, 103501 (2000) [arXiv:hep-ph/9910214]; S. Tsujikawa

and H. Yajima, Phys. Rev. D **62**, 123512 (2000) [arXiv:hep-ph/0007351].

[27] A. R. Liddle and D. H. Lyth, *Cosmological inflation and large-scale structure*, Cambridge University Press (2000).

[28] D. I. Kaiser, Phys. Rev. D **53**, 1776 (1996) [arXiv:astro-ph/9507108].

[29] P. B. Greene, L. Kofman, A. D. Linde and A. A. Starobinsky, Phys. Rev. D **56**, 6175 (1997) [arXiv:hep-ph/9705347].

[30] H. V. Peiris *et al.*, Astrophys. J. Suppl. **148**, 213 (2003); V. Barger, H. S. Lee, and D. Marfatia, Phys. Lett. B **565**, 33 (2003) [arXiv:hep-ph/0302150]; W. H. Kinney, E. W. Kolb, A. Melchiorri and A. Riotto, Phys. Rev. D **69**, 103516 (2004) [arXiv:hep-ph/0305130]; S. M. Leach and A. R. Liddle, Phys. Rev. D **68**, 123508 (2003) [arXiv:astro-ph/0306305]; S. Tsujikawa and A. R. Liddle, JCAP **0403**, 001 (2004) [arXiv:astro-ph/0312162]; S. Tsujikawa and B. Gumjudpai, Phys. Rev. D **69**, 123523 (2004) [arXiv:astro-ph/0402185].